ChemComm
Chemical Communications

Accepted Manuscript

This article can be cited before page numbers have been issued, to do this please use: M. Tian, C. Liu, B. Dong, Y. Zuo and W. Lin, *Chem. Commun.*, 2019, DOI: 10.1039/C9CC03679B.

ROYAL SOCIETY OF CHEMISTRY

rsc.li/chemcomm

View Article Online
DOI: 10.1039/C9CC03679B

COMMUNICATION

A dual-site controlled ratiometric probe revealing the simultaneous down-regulation of pH in lysosomes and cytoplasm during autophagy

Received 00th January 20xx,
Accepted 00th January 20xx

DOI: 10.1039/x0xx00000x

Minggang Tian, Chuang Liu, Baoli Dong, Yujing Zuo, and Weiying Lin*

In this work, a unique dual-site controlled fluorescent probe was presented for the sensitive and concurrent detection of pH in cytoplasm and lysosomes. With the probe, the simultaneous down-regulation of pH in lysosomes and cytoplasm during autophagy has been successfully revealed for the first time.

Autophagy is a significant pathway for live cells to degrade unwanted components including proteins and organelles.[1] Autophagy has attracted intense focus in recent years, owning to its indispensable roles in infection, self-repairing, programmed cell death, and some other biological and pathological processes.[2-3] Abnormal regulation of autophagy is implicated in many severe diseases such as Pakinson disease and cancer.[4-5] During the autophagy process, the substrates in cytoplasm are transported into lysosomes and digested.[6] Lysosomal and cytoplasm pH plays complex roles in autophagy process, and for example, the raise of lysosomal pH could efficiently inhibit autophagy by decreasing the activity of hydrolase.[7] Researches also prove that the acidic pH environments can induce and promote the autophagy levels.[8] Therefore, monitoring pH changes in cytoplasm and lysosomes during autophagy is of fundamental significance for the investigation on the internal relationship between pH and autophagy, and promoting the in-depth understanding of autophagy.

Nowadays, colormetric analysis, electrochemical, and other methods have been applied in the detection of pH values.[9-10] In comparison with these techniques, fluorescence microscopy displays superior advantages.[11] With suitable fluorescent probes, the intracellular pH could be mapped at micrometer scale. The dynamic pH changes in live cells can be in-situ and real-time visualized under fluorescence microscope. To realize the fluorescence imaging of intracellular pH, many kinds of fluorescent probes have been constructed with various response sites and fluorescence mechanisms.[12-13] For example, Urano *et al.* have presented a near-infrared fluorescent probe for pH in acid compartments using piperazine as the response group, working on photo-induced electron transfer (PET) mechanism.[14] Kim and co-workers have developed fluorescent probes for ratiometric detection of lysosomal pH based on imidazole group.[15] Yu *et al.* have reported a fluorescent probe for mitochondrial pH with a hydroxyl group as the recognition site.[16]

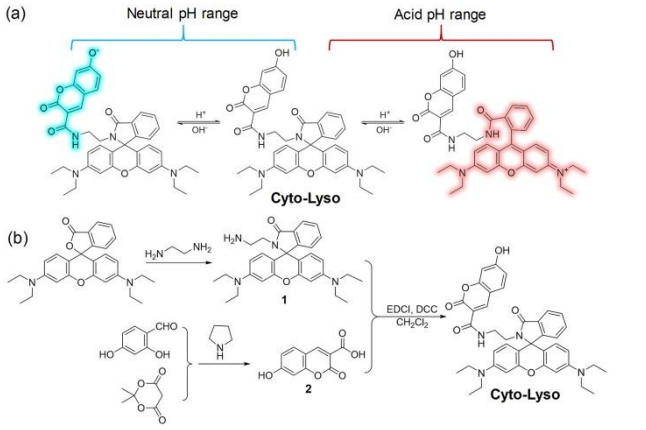

Scheme 1. The sensing mechanism of **Cyto-Lyso** to pH in neutral and acid ranges (a); the synthetic routine of **Cyto-Lyso** (b).

To investigate the pH change in cytoplasm and lysosomes during autophagy, fluorescent probes targeting both lysosomes and cytoplasm and sensitive to pH in neutral and acid range are in urgent need. A possible strategy is to develop dual-site controlled pH probes. Tang *et al.* have reported a dual-site fluorescent probe for intracellular pH values, but the probe was insensitive to pH in the acid range (4.5-5.5), which limited its application in detecting lysosomal pH.[17] Our group has also designed a dual-site fluorescent probe for ratiometric detection of lysosomal pH.[18] The probe exclusively target lysosomes due

Institute of Fluorescent Probes for Biological Imaging, School of Chemistry and Chemical Engineering, School of Materials Science and Engineering, University of Jinan, Jinan, Shandong 250022, People's Republic of China. E-mail: weiyinglin2013@163.com.

Electronic Supplementary Information (ESI) available: [Synthesis of the probe, absorption and fluorescence spectra, characterization data]. See DOI: 10.1039/x0xx00000x

to the basic properties of morpholine and piperazine, and thus cannot be used to image cytoplasm pH. Up to now, fluorescent probes enabling the simultaneous visualization of pH in cytoplasm and lysosomes have not been reported yet.

Consequently, the probe should exhibit two sites to sense the pH in neutral and acid range for cytoplasm and lysosomes, respectively, and distributed in lysosomes and cytoplasm. In this work, as presented in Scheme 1a, 7-hydroxyl-coumarin moiety was selected for the neutral pH range, and amino-rhodamine part was used for the acid pH. Meanwhile, amide group with weak basic properties was decorated onto the probe, to ensure that the probe can target both lysosomes and cytoplasm. As a result, the probe **Cyto-Lyso** targets both cytoplasm and lysosomes, and enables the ratiometric detection of pH in the two locations with high sensitivity. The down-regulation of pH values in cytoplasm and lysosomes have been successfully revealed, and the inhibition of NH_4Cl and chloroquine (CQ) to autophagy has been evidently observed by means of the probe.

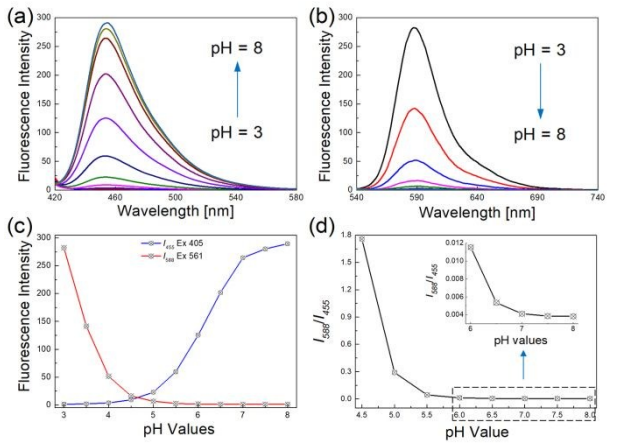

Figure 1. The emission spectra of 10 μM **Cyto-Lyso** under different pH values with the excitation of 405 nm (a) and 500 nm (b); the pH-dependent fluorescence intensity at 455 nm (excited by 405 nm) and 588 nm (excited by 500 nm) (c); the pH-dependent intensity ratio of 588 nm to 455 nm, insert: amplification at pH values of 6.0 ~ 8.0.

The optical properties of **Cyto-Lyso** were acquired initially to confirm its response to different pH values. As depicted in Figure 1a, **Cyto-Lyso** displayed very weak blue emission at the pH of 3, and the fluorescence intensity sharply increased by ~ 230-fold when the pH value changed from 3.0 to 8.0. Meanwhile, **Cyto-Lyso** showed strong red fluorescence at the pH of 3.0, which was nearly disappeared when the pH was changed to 8.0. The pH-dependent fluorescence intensity at 455 nm and 588 nm was plotted in Figure 1c. From the results, the pK_a values of the two response parts were calculated as 3.5 and 6.2, respectively. Consequently, the two sensing sites could be used to assess the pH values at acid and neutral range, respectively. To testify the ability of **Cyto-Lyso** in ratiometric detection of pH values, the red-to-blue intensity ratio was also calculated, as plotted in Figure 1d. Since the physiological range generally distributed in the range of 4.5~8.0, the pH-dependent ratio was plotted in the range. As displayed in Figure 1d and the insert, the intensity ratio decreased from 1.76 to 0.04 when the pH changed from 4.5 to 5.5, implying the ability of **Cyto-Lyso** to ratiometrically image the pH change in acid range of lysosomes. Moreover, the intensity ratio decreased from 0.012 to 0.004 when the pH changed from 6.0 to 8.0, indicating that **Cyto-Lyso** can detect pH change in neutral range of cytoplasm.

The interferences from various bioreagents including heavy metals, biological ions, phosphates, etc. have been testified as shown in Figure S1. Obviously, these reagents would not induce evident change to the fluorescence of **Cyto-Lyso**, confirming the high selectivity of the probe to pH values.

The cytotoxicity of **Cyto-Lyso** was consequently testified before the cell imaging experiments. As shown in Figure S2a, the survival rates of HepG2 cells incubated with 5 μM **Cyto-Lyso** for 2 h, 12 h, and 24 h are 99.5%, 96.0%, and 94.3%, respectively. Moreover, the viability of live cells incubated with 5-30 μM **Cyto-Lyso** for 12 h is above 85 % (Figure S2b), indicating the low cytotoxicity of the probe. In cell imaging experiments, live HepG2 cells were incubated with 5 μM **Cyto-Lyso** for 30 min, and the cytotoxicity could be ignored under the experimental conditions.

The photostability of **Cyto-Lyso** in cells was also investigated in-situ with the ceaseless irradiation of 405 nm and 561 nm lasers. In Figure S3, after the irradiation for 16 min, intense intracellular emission was still detected and the fluorescence bleaching could be ignored. These results demonstrated the high photostability of **Cyto-Lyso**, which was potential for the long-term imaging of live cells.

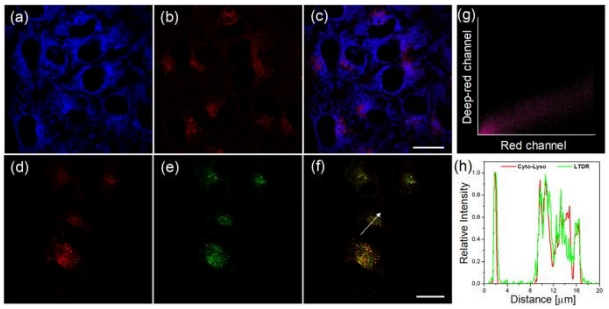

Figure 2. The fluorescence images of live HepG2 cells incubated with 5 μM **Cyto-Lyso** for 30 min (a-c) or co-stained with 5 μM **Cyto-Lyso** and 200 nM LTDR for 30 min (d-f); the co-localization scatter plot (g); the intensity distribution of **Cyto-Lyso** and **LTDR** along the arrow in Figure 2f. Bar = 20 μm.

Live HepG2 cells were then incubated and imaged with the probe **Cyto-Lyso**, as shown in Figure 2a-2c. Evidently, **Cyto-Lyso** displayed intense blue and weak red fluorescence in live HepG2 cells. Observed from the merged images, the red and blue fluorescent signals localized in different compartments in cells. The red signals presented in small dots which is in accordance with the lysosomal morphology. Considering that strong red emission only exists in acid conditions, the red signals may localized in lysosomes. To confirm this speculation, the red signals of **Cyto-Lyso** were co-localized with **LTDR**, a commercialized fluorescent probe for lysosomes. As presented in Figure 2d-2f, the red signals of **Cyto-Lyso** overlapped well with the **LTDR** shown in green pseudo color, and the co-localization coefficient was up to 0.89. Moreover, according to the scattering plot and spatial distribution of **Cyto-Lyso** and **LTDR**, the two probes co-localized well in live HepG2 cells. Thus,

red signals from **Cyto-Lyso** actually localized in lysosomes. Moreover, in Figure 2a, the blue signals from **Cyto-Lyso** distributed in the cytoplasm. Co-localization experiments of **Cyto-Lyso** with **ERTR** and **MTDR**, commercial probes for endoplasmic reticulum (ER) and mitochondria, were performed. In Figure S4, the blue signals of **Cyto-Lyso** well overlapped with ERTR and partially overlapped with MTDR, and the Pearson's coefficients were 0.85 and 0.65, respectively. These results indicate that **Cyto-Lyso** mainly localized in ER. The ER membrane is highly permeable to protons,[19] and ER pH is the same as the cytoplasm. Consequently, **Cyto-Lyso** could image cytoplasm pH.

The response of **Cyto-Lyso** to intracellular pH was then confirmed. Live HepG2 cells were incubated by culture medium with different pH values. The nutritious culture medium can block the autophagy, and the different pH of the culture medium would alter the intracellular pH values. In Figure S5, compared with the cells cultured in normal culture medium (pH 7.2-7.4), cells treated at the pH of 8.0 showed evidently enhanced emission in blue channel and decreased fluorescence in red channel, indicating that **Cyto-Lyso** could image the arised pH in cells. In comparison, the cells treated in the pH of 7.0, 6.0, 5.0, and 4.0 displayed gradually decreased blue fluorescence and enhanced red emission, confirming that **Cyto-Lyso** could image the pH changes in cells. Ratiometric images were also obtained, and the pseudo colors were given according to the color bar. In Figure S5, with the pH of the culture medium changing from 8.0 to 4.0, the pseudo colors in the ratiometric image changed from green to red, demonstrating the increase of the ratio. Therefore, **Cyto-Lyso** can image intracellular pH changes in a ratiometric manner.

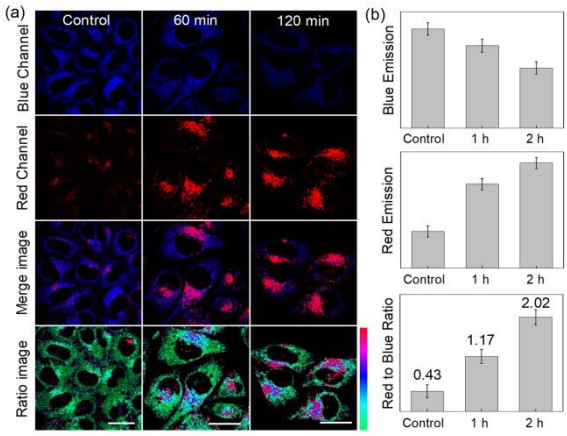

Figure 3. The fluorescent images of HepG2 cells pre-stained with 5 μM **Cyto-Lyso** for 30 min (a) then incubated with culture medium for 120 min (Control) and PBS buffer for 60 min and 120 min. The mean intensity in blue channel, red channel, and the intensity ratio of red to blue channel of the three groups of cells. Bar = 20 μm.

The pH changes in cytoplasm and lysosomes during autophagy were afterwards investigated with the probe **Cyto-Lyso**. Nutrient starvation conditions can induce the autophagy,[20,21] and therefore live HepG2 cells were stained with the probe then incubated by PBS buffer for 60 min and 120 min, respectively. Western Blotting (WB) experiments were performed to confirm the activation of autophagy under starvation conditions. As presented in Figure S6, the Atg-7 protein overexpressed under the starvation for 2 h, indicating the activation of autophagy. In Figure 3a, HepG2 cells in the culture medium showed intense fluorescence in blue channel, and weak emission in red channel. By contrast, the cells after the starvation for 60 min showed slightly decreased blue emission, and largely enhanced red emission, indicating the slightly decreased pH in cytoplasm and largely decreased pH in lysosomes, respectively. The pH changes could be clearly observed from the ratiometric images. According to the results in Figure S5, the cytoplasm pH decreased to ~7.0, and the lysosomal pH decreased to ~5.0. The cells after the starvation for 120 min were also imaged with **Cyto-Lyso**. In Figure 3a, compared with the cells starved for 60 min, these cells showed evidently decreased emission in the blue channel, and further enhanced fluorescence in the red channel. Ratiometric images were also acquired, and the cytoplasm pH was in the range of 6.0~7.0 in these cells, while the lysosomal pH was in 4.0~5.0. These results demonstrated that both the cytoplasm pH and lysosomal pH actually decreased during the autophagy process.To clearly assess the pH changes in cytoplasm and lysosomes during autophagy, the mean intensity in blue and red channels and their ratio have been calculated in Figure 3b. The decreased blue emission intensity could be evidently observed, and the red to blue ratio was also dramatically changed during the autophagy process. These results also demonstrated the decreased pH in neutral and acid range during autophagy.

The pH changes in 4T1 cells during autophagy were also investigated with the probe **Cyto-Lyso** to check the universality, as displayed in Figure S7. Similar to the HepG2 cells, 4T1 cells cultured in the culture medium showed intense blue fluorescence and weak red emission. After the starvation for 60 min, the fluorescence in the blue channel slightly decreased, and the emission in the red channel evidently increased. In comparison the results in Figure S5, the cytoplasm pH was around 7.0, and the lysosomal pH was in the range of 5.0~6.0. The starvation time was also prolonged, and obviously decreased blue emission and further increased red fluorescence could be observed. The cytoplasm pH was in the range of 6.0~7.0, and the lysosomal pH changed to ~5.0. Therefore, the cytoplasm and lysosomal pH of 4T1 cells decreased during the starvation induced procedure.The mean intensity in two channels and their ratio were also calculated as presented in Figure S7b. The decreased emission in blue channel and enhanced fluorescence in red channel could be clearly observed. Moreover, the red to blue ratio in 4T1 cells steadily increased during starvation. These results also demonstrated the decreased pH in both neutral and acid range during autophagy.

CQ was reported as an inhibitor of the autophagy process,[22] and the effect of CQ on autophagy was investigated. As shown in Figure 4, after the starvation treatment in buffer containing 25 μM CQ, the autophagy has been slightly suppressed. Meanwhile, the weak emission in cytoplasm indicating the decreased pH in cytoplasm during autophagy. The lysosomal pH increased compared with the cells treated in buffer without CQ for 120 min (Figure 3), which should be attributed to the CQ-caused lysosomal alkalization. With the increase of CQ

concentration, the proportion of lysosomes obviously decreased, indicating evident inhibition of autophagy. Notably, the cytoplasm emission obviously enhanced with the elevated CQ concentration, indicating that the increase of cytoplasm pH is accompanied with autophagy inhibition.

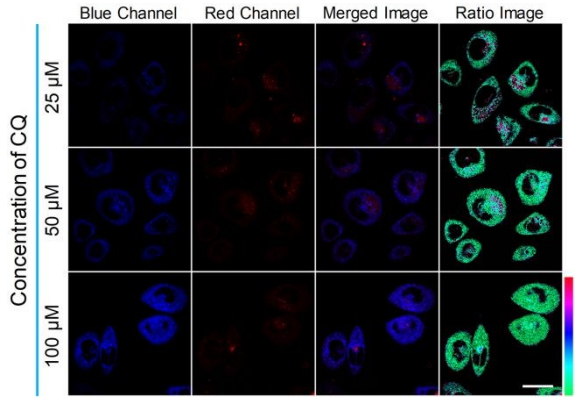

Figure 4. The fluorescence images of HepG2 cells pre-stained with 5 μM **Cyto-Lyso** for 30 min (a) then incubated in PBS containing different amount of CQ for 2 h. Bar = 20 μm.

NH_4Cl has been reported to cause the increase of intracellular pH,[23] and the effect of NH_4Cl on autophagy was also studied in Figure S8. Compared with the cells starved for 2 h, addition of 50 μM NH_4Cl would not bring obvious effect on autophagy. However, the cytoplasm pH is apparently increased compared with the groups without NH_4Cl. Consequently, 50 μM NH_4Cl can induce pH elevation in cytoplasm, but cannot inhibit autophagy. In comparison, 100 μM or 200 μM NH_4Cl could efficiently inhibit the autophagy, and caused the increase of cytoplasm and lysosomal pH. WB experiments were performed to demonstrate the inhibition of NH_4Cl to autophagy. In Figure S6, the expression of Atg-7 protein of cells treated by 100 μM NH_4Cl decreased, compared with cells starved in PBS buffer, indicating the inhibition of autophagy process. Overall, the cytoplasm and lysosomal pH is decreased during autophagy. The cytoplasm alkalization brings little influence on autophagy, while the elevated lysosomal pH may inhibit autophagy.

Conclusions

In summary, a dual-site fluorescent probe (**Cyto-Lyso**) for the ratiometric imaging of cytoplasm and lysosomal pH values with high sensitivity has been constructed. For molecular design, 7-hydroxyl-coumarin moiety was used to detect cytoplasm pH, and amino-rhodamine was utilized to sense lysosomal pH. The probe target both lysosomes and cytoplasm, and could image pH in the dual targets with high sensitivity. The concurrently down-regulation of pH in cytoplasm and lysosomes was successfully revealed in a ratiometric manner during the starvation induced autophagy. The inhibition effect of NH_4Cl and CQ on autophagy have been also investigated with the probe. The probe can serve as a valid tool for the assessment of pH changes in cytoplasm and lysosomes simultaneously, and facilitate the fundamental researches on autophagy and relative areas.

Conflicts of interest

View Article Online
DOI: 10.1039/C9CC03679B

There are no conflicts to declare.

Acknowledgement

For financial support, we thank the National Natural Science Foundation of China (NSFC) (21472067, 21672083, 21877048, 21804052), the Taishan Scholar Foundation (TS201511041), the Natural Science Foundation of Shandong Province (ZR2018BB058), and the startup funds of University of Jinan (309-10004, 160100331).

Notes and references

1 Mizushima, N.; Komatsu, M., *Cell* **2011,** *147* (4), 728-741.
2 Thurston, T. L. M.; Wandel, M. P.; von Muhlinen, N.; Foeglein, Á.; Randow, F., *Nature* **2012,** *482*, 414.
3 Cuervo, A. M.; Bergamini, E.; Brunk, U. T.; Dröge, W.; Ffrench, M.; Terman, A., *Autophagy* **2005,** *1* (3), 131-140.
4 Kitada, T.; Asakawa, S.; Hattori, N.; Matsumine, H.; Yamamura, Y.; Minoshima, S.; Yokochi, M.; Mizuno, Y.; Shimizu, N., *Nature* **1998,** *392*, 605.
5 Jin, S.; White, E., *Autophagy* **2007,** *3* (1), 28-31.
6 Eskelinen, E.-L.; Saftig, P., *Biochim. Biophysic. Acta* **2009,** *1793* (4), 664-673.
7 Filomeni, G.; De Zio, D.; Cecconi, F., *Cell Death Differentiation* **2014,** *22*, 377.
8 Devin M. W.; Ju-hyun L.; Asok K.; Sooyeon L.; Samantha J. O.; Ralph A. N.,. *Eur. J. Neur.* **2013,** *37* (22), 1949-1961.
9 Wang, Y.; Tang, B.; Zhang, S., *Dyes Pigments* **2011,** *91* (3), 294-297.
10 Zhou, J.; Zhang, L.; Tian, Y., *Anal. Chem.* **2016,** *88* (4), 2113-2118.
11 Chen, H.; Dong, B.; Tang, Y.; Lin, W.,. *Acc. Chem. Res.* **2017,** *50* (6), 1410-1422.
12 Lee, M. H.; Park, N.; Yi, C.; Han, J. H.; Hong, J. H.; Kim, K. P.; Kang, D. H.; Sessler, J. L.; Kang, C.; Kim, J. S., *J. Am. Chem. Soc.* **2014,** *136* (40), 14136-14142.
13 Hou, J.-T.; Ren, W. X.; Li, K.; Seo, J.; Sharma, A.; Yu, X.-Q.; Kim, J. S., *Chem. Soc. Rev.* **2017,** *46* (8), 2076-2090.
14 Takahashi, S.; Kagami, Y.; Hanaoka, K.; Terai, T.; Komatsu, T.; Ueno, T.; Uchiyama, M.; Koyama-Honda, I.; Mizushima, N.; Taguchi, T.; Arai, H.; Nagano, T.; Urano, Y., *J. Am. Chem. Soc.* **2018,** *140* (18), 5925-5933.
15 Kim, H. J.; Heo, C. H.; Kim, H. M., *J. Am. Chem. Soc.* **2013,** *135* (47), 17969-17977.
16 Wu, M.-Y.; Li, K.; Liu, Y.-H.; Yu, K.-K.; Xie, Y.-M.; Zhou, X.-D.; Yu, X.-Q., *Biomaterials* **2015,** *53*, 669-678.
17 Chen, S.; Hong, Y.; Liu, Y.; Liu, J.; Leung, C. W. T.; Li, M.; Kwok, R. T. K.; Zhao, E.; Lam, J. W. Y.; Yu, Y.; Tang, B. Z., *J. Am. Chem. Soc.* **2013,** *135* (13), 4926-4929.
18 Dong, B.; Song, X.; Wang, C.; Kong, X.; Tang, Y.; Lin, W., *Anal. Chem.* **2016,** *88* (7), 4085-4091.
19 Kim, J.; Johannes, L.; Goud, B.; Antony, C.; Lingwood, C.; Daneman, R.; Grinstein, S., *Proc. Natl. Acad. Sci.* 1997, **95**, 2997-3002.
20 Mizushima, N.; Yamamoto, A.; Matsui, M.; Yoshimori, T.; Ohsumi, Y., *Mol. Biol. Cell* **2004,** *15* (3), 1101-1111.
21 Jiang, J.; Tian, X.; Xu, C.; Wang, S.; Feng, Y.; Chen, M.; Yu, H.; Zhu, M.; Meng, X., *Chem. Commun.* 2017, **53**, 3645-3648.
22 Liang, D. H.; Choi, D. S.; Ensor, J. E.; Kaipparettu, B. A.; Bass, B. L.; Chang, J. C., *Cancer Lett.* **2016,** *376* (2), 249-258.
23 Hagag, N.; Lacal, J. C.; Graber, M.; Aaronson, S.; Viola, M. V., *Mol. Cell. Biol.* **1987,** *7* (5), 1984-1988.